

Alma Mater Studiorum Università di Bologna
Archivio istituzionale della ricerca

Estimation for multivariate normal rapidly decreasing tempered stable distributions

This is the final peer-reviewed author's accepted manuscript (postprint) of the following publication:

Published Version:

Bianchi, M.L., Tassinari, G.L. (2023). Estimation for multivariate normal rapidly decreasing tempered stable distributions. JOURNAL OF STATISTICAL COMPUTATION AND SIMULATION, 94(1), 103-125 [10.1080/00949655.2023.2232913].

Availability:

This version is available at: <https://hdl.handle.net/11585/945259> since: 2023-10-16

Published:

DOI: <http://doi.org/10.1080/00949655.2023.2232913>

Terms of use:

Some rights reserved. The terms and conditions for the reuse of this version of the manuscript are specified in the publishing policy. For all terms of use and more information see the publisher's website.

This item was downloaded from IRIS Università di Bologna (<https://cris.unibo.it/>).
When citing, please refer to the published version.

(Article begins on next page)

This is the final peer-reviewed accepted manuscript of:

Michele Leonardo Bianchi & Gian Luca Tassinari (2024) Estimation for multivariate normal rapidly decreasing tempered stable distributions, Journal of Statistical Computation and Simulation, 94:1, 103-125.

The final published version is available online at:

<https://doi.org/10.1080/00949655.2023.2232913>

Terms of use:

Some rights reserved. The terms and conditions for the reuse of this version of the manuscript are specified in the publishing policy. For all terms of use and more information see the publisher's website.

This item was downloaded from IRIS Università di Bologna (<https://cris.unibo.it/>)

When citing, please refer to the published version.

Estimation for multivariate normal rapidly decreasing tempered stable distributions

Michele Leonardo Bianchi^{a,*1}, Gian Luca Tassinari^b

^a*Financial Stability Directorate, Bank of Italy,
micheleleonardo.bianchi@bancaditalia.it*

^{*} Corresponding author

^b*Department of Management,
University of Bologna,
gianluca.tassinari2@unibo.it*

This version: June 28, 2023

Abstract. In this paper we describe a methodology for parameter estimation of multivariate distributions defined as normal mean-variance mixture where the mixing random variable is rapidly decreasing tempered stable distributed. We address some numerical issues resulting from the use of the characteristic function for density approximation. We focus our attention on the practical implementation of numerical methods involving the use of these multivariate distributions in the field of finance and we empirically assess the proposed algorithm through an analysis on a five-dimensional series of stock index log-returns.

JEL Classification: C58; G10; G21; G32.

Key words: tempered stable random variable, rapidly decreasing tempered stable random variable, expectation-maximization, maximum likelihood estimation, non-Gaussian models.

¹ The authors are grateful to four anonymous referees for their helpful suggestions. The views expressed are those of the authors and do not necessarily reflect those of the Bank of Italy.

1 Introduction

The tempered infinitely divisible (TID) class of random variables introduced by Bianchi et al. [2011] has the same desirable properties as the tempered stable (TS) class defined in the seminal work of Rosinski [2007] (see also Grabchak [2016]), but with the advantage that it may admit exponential moments of any order. More precisely, in some cases the characteristic function of a TID random variable is extendible to an entire function on \mathbb{C} , that is, it admits any exponential moment. As observed in Bianchi et al. [2011], some practical problems in the field of mathematical finance have motivated the study of TID random variables. Specifically, Bianchi et al. [2011] sought a discrete-time option pricing model that accounts for well-known stylized facts observed about real-world stock market returns: asymmetry, time-varying variance, and heavy tails.

The rapidly decreasing tempered stable (RDTS) random variable was originally proposed in Bianchi et al. [2011] and extended by Fallahgoul et al. [2019] and Fallahgoul and Loeper [2021] to a multivariate framework by considering a normal mean-variance mixture approach with a RDTS subordinator. Recently, Grabchak [2021] proposed an exact simulation method for RDTS random variables to alleviate the difficulties connected to their practical use.

Over the past few years, RDTS models have proven to be useful for application to finance. Readers are referred to Bianchi et al. [2019] to have a full understanding on how these models can be used in financial applications such as risk management, option pricing, and other related areas. As observed above, based on the property that a RDTS random variable admits any exponential moment, Kim et al. [2010] defined a RDTS-GARCH option pricing model without artificially restricting the variance process as in the classical tempered stable (CTS) case. Bianchi [2015] empirically studied the shape of the RDTS density function, demonstrating that the RDTS density is much closer to the CTS density than to the normal one, even if the RDTS random variable has exponential moments of any order as the normal random variable. Kim et al. [2019] presented an option pricing model for a RDTS Lévy process with long-range dependence. Fallahgoul et al. [2019] proposed a bivariate model based on a RDTS subordinator to price quanto options, and Fallahgoul and Loeper [2021] analyzed a bivariate time-series of indexes log-returns by replacing the physical time of the Brownian motion with a RDTS stochastic clock. This latter approach, also known as stochastic time-change, has been widely studied in the literature on stochastic models applied to finance (see Luciano and Semeraro [2010], Buchmann et al. [2017] and Fallahgoul et al. [2021]).

As remarked by Xia and Grabchak [2022], it is not simple to work with the spectral measure defined in the influential paper of Rosinski [2007]. Even if in the more general setting the spectral measure provides a greater flexibility, since the tail behaviour depends on the direction on the hypersphere in \mathbb{R}^n , it is still not clear how to estimate this spectral measure when the dimension is greater than two. For this reason, in this work we consider a multivariate distribution defined as a normal mean-variance mixture in which the mixing random variable is RDTS distributed and we refer to this model as the multivariate normal rapidly decreasing tempered stable (MNRDTS) model. In this paper we show how to estimate the parameters of a MNRDTS distribution through an extension of the expectation-maximization (EM) maximum likelihood estimation (MLE) method of Dempster et al. [1977], which is particularly convenient as it allows to find the

parameters of the multivariate Gaussian distribution and those of the mixing distribution separately, as shown in Protasov [2004] and Hu [2005] in the multivariate generalized hyperbolic (MGH) case, and in Bianchi et al. [2016] in the multivariate normal tempered stable case (MNTS). The evaluation of the characteristic function of a RDTS random variable or of the margins of a MNRDTS distribution is not a simple task, because it involves the evaluation of a confluent hypergeometric (or Kummer) function. We show how to deal with this problem in an efficient way and we empirically assess our estimation algorithm by considering the time-series of the main five euro area stock indexes.

It should be noted that, differently from the MNTS case, the characteristic function of the margins of a MNRDTS random variable is an entire function, because it can be viewed as a composition of entire functions. This properties seems particularly useful in applications to finance (see for example Broda and Zambrano [2021]) requiring that the characteristic function be analytic in a strip containing the real axis in its interior.

The paper is organized as follows. The multivariate model analyzed in this work is defined in Section 2. In Section 3.1 we show how to estimate the model parameters through an extension of the EM-MLE approach and we identify some computational issues in the evaluation of the characteristic function of a MNRDTS random variable. In Section 4 we describe the data analyzed in the empirical study and we discuss the main empirical results. Finally, in Section 5 we conduct a simulation study to assess the EM-based algorithm performance. Section 6 concludes.

2 The model

Let $Y = \{Y_t, t \geq 0\}$ be an n -dimensional process defined as

$$Y_t = \mu t + \theta S_t + D_\sigma W_{S_t}, \quad (2.1)$$

where $S = \{S_t, t \geq 0\}$ is a *one*-dimensional subordinator, $W = \{W_t, t \geq 0\}$ is an n -dimensional Wiener process with $\text{corr}[W_{j,t}, W_{k,t}] = \rho_{jk}$, independent from S , μ and θ are two n -dimensional vectors containing real parameters, D_σ is a diagonal matrix of order n with diagonal elements $\sigma_j > 0$, with $j = 1, \dots, n$.

For each discrete time step, Δt , the distribution of the increments of the process belongs to the normal mean-variance mixture family

$$Y_{\Delta t} = \mu \Delta t + \theta S_{\Delta t} + \sqrt{S_{\Delta t}} D_\sigma A Z, \quad (2.2)$$

where Z is a vector of n independent standardized Gaussian random variables, $S_{\Delta t}$ denotes the distribution of the subordinator increments where $S_{\Delta t} \perp Z$, A is the lower Cholesky decomposition of a correlation matrix Ω , that is, $\Omega^{1/2} = A$ and $D_\sigma A = \Sigma^{1/2}$. The characteristic function of Y_t defined in equation (2.1) is given by

$$\Psi_{Y_t}(u) = \exp(itu' \mu + tl_{S_1}(\varphi(u))), \quad (2.3)$$

where $l_{S_1}(\cdot)$ is the Laplace exponent of the subordinator, and $\varphi(u)$ is the characteristic exponent of the multivariate Brownian motion, that is

$$\begin{aligned} \varphi(u) &= iu' \theta - \frac{1}{2} u' \Sigma u \\ &= \sum_{j=1}^n iu_j \theta_j - \frac{1}{2} \sum_{j=1}^n \sum_{k=1}^n u_j u_k \sigma_j \sigma_k \rho_{jk}, \end{aligned} \quad (2.4)$$

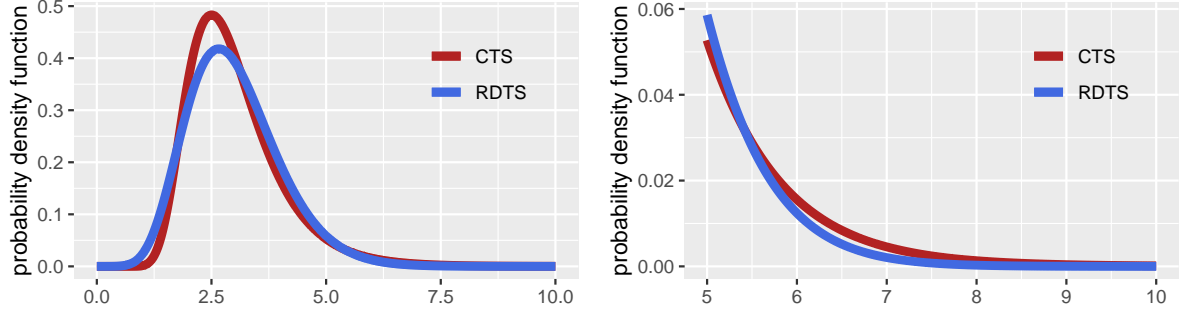


Figure 1: Probability density function of CTS and RDTs subordinators with parameter $\alpha = 0.75$, expected value equal to 3 and unit variance.

where $u \in \mathbb{R}^n$ and the matrix Σ has elements $\Sigma_{jk} = \sigma_j \sigma_k \rho_{jk}$. Since Σ is a variance-covariance matrix, we can rewrite equation (2.4) using matrix notation, as follows

$$\varphi(u) = iu'\theta - \frac{1}{2}u'D_\sigma\Omega D_\sigma u,$$

where D_σ is a diagonal matrix with diagonal $\sigma \in \mathbb{R}_+^n$, and Ω is the correlation matrix of the Brownian motions with elements ρ_{jk} .

A process $S = \{S_t, t \geq 0\}$ with Lévy measure given by

$$\nu(dx) = C \frac{e^{-\frac{\lambda^2 x^2}{2}}}{x^{\alpha+1}} I_{x>0} dx, \quad (2.5)$$

where $\lambda > 0$, $C > 0$, $0 < \alpha < 1$ and Lévy triplet $(0, \nu, 0)$ is said to be a RDTs subordinator. Recall that the Lévy measure of a CTS subordinator is given by

$$\nu(dx) = C \frac{e^{-\lambda x}}{x^{\alpha+1}} I_{x>0} dx.$$

In Figure 1 we show the probability density function of CTS and RDTs subordinators with parameter $\alpha = 0.75$, expected value equal to 3 and unit variance. The right tail of the RDTs subordinator goes faster to zero with respect to the CTS one. Readers are referred to the Appendix A.1, to Bianchi et al. [2019] and Bianchi et al. [2022] for the moments formulas.

The characteristic function of S_t is given by

$$\Psi_{S_t}(u) = E[\exp(iuS_t)] = \exp\left(t 2^{-\frac{\alpha}{2}-1} C \lambda^\alpha G(iu; \alpha, \lambda)\right), \quad (2.6)$$

where

$$\begin{aligned} G(x; \alpha, \lambda) = & \Gamma\left(-\frac{\alpha}{2}\right) \left(M\left(-\frac{\alpha}{2}, \frac{1}{2}; \frac{x^2}{2\lambda^2}\right) - 1 \right) + \\ & + \frac{\sqrt{2}x}{\lambda} \Gamma\left(\frac{1-\alpha}{2}\right) M\left(\frac{1-\alpha}{2}, \frac{3}{2}; \frac{x^2}{2\lambda^2}\right), \end{aligned} \quad (2.7)$$

where $M(a, b; z)$ is the confluent hypergeometric (or Kummer) function of the first kind as defined in equation (13.1.2) in Abramowitz and Stegun [1974], that is

$$M(a, b; z) = 1 + \frac{az}{b} + \frac{(a)_2 z^2}{(b)_2 2!} + \cdots + \frac{(a)_n z^n}{(b)_n n!}, \quad (2.8)$$

where

$$(m)_n = m(m+1)(m+2) \dots (m+n-1),$$

with $m \in \mathbb{R}$. It follows that $\phi_{S_t}(u)$ is an entire function on \mathbb{C} .

As shown in the Appendix A.3, equation (2.7) can be written in terms of the confluent hypergeometric function of the second kind, i.e. the special function $U(a, b; z)$,

$$G(x; \alpha, \lambda) = -\Gamma\left(-\frac{\alpha}{2}\right) + \pi^{-\frac{1}{2}} \Gamma\left(\frac{1-\alpha}{2}\right) \Gamma\left(-\frac{\alpha}{2}\right) U\left(-\frac{\alpha}{2}, \frac{1}{2}; \frac{x^2}{2\lambda^2}\right). \quad (2.9)$$

This second representation is useful in the computation involving the characteristic function of the MNRDTS random variable (see equation (2.11)).

For a more simple derivatives computation, by the definition of the function M , the function G can be written as

$$2^{-\frac{\alpha}{2}-1} \lambda^\alpha G(x; \alpha, \lambda) = \frac{1}{2} \sum_{n=2}^{\infty} \frac{x^n}{n!} \left(\frac{\lambda}{\sqrt{2}}\right)^{\alpha-n} \Gamma\left(\frac{n-\alpha}{2}\right). \quad (2.10)$$

This is useful to compute the moments of the RDTS subordinator (see the Appendix A.1).

From equation (2.6) it is possible to compute the Laplace exponent of the RDTS subordinator

$$l_{S_t}(u) = \ln \phi_{S_t}(-iu) = t 2^{-\frac{\alpha}{2}-1} C \lambda^\alpha G(u; \alpha, \lambda),$$

and using (2.3) we get the characteristic function of the MNRDTS process with linear drift

$$\Psi_{Y_t}(u) = \exp\left(itu'\mu + t 2^{-\frac{\alpha}{2}-1} C \lambda^\alpha G\left(iu'\theta - \frac{1}{2}u'\Sigma u; \alpha, \lambda\right)\right). \quad (2.11)$$

Setting $u_i = 0, \forall i \neq j$, into (2.11) we get the characteristic function of the j -th marginal distribution

$$\Psi_{Y_{j,t}}(u_j) = \exp\left(itu_j\mu_j + t 2^{-\frac{\alpha}{2}-1} C \lambda^\alpha G\left(iu_j\theta_j - \frac{1}{2}u_j^2\sigma_j^2; \alpha, \lambda\right)\right). \quad (2.12)$$

The moments of this multivariate random variable are reported in the Appendix A.2.

3 Parameter estimation

After having defined the MNRDTS model, we show how to deal with its estimation. In Section 3.1 we describe the algorithm to estimate the parameters of the MNRDTS distribution. Then, we show how to evaluate the characteristic function in equation (2.6) (see Section 3.2).

3.1 Expectation-conditional maximization either algorithm

A direct MLE for the n -dimensional multivariate model described in Section 2 is not feasible, since the number of parameters to be estimated is $(n^2 + 5n)/2 + 3$. The matrix Σ has $(n^2 + n)/2$ elements, the vectors μ and θ have n elements, and there are the three parameters of the subordinator S (i.e. α , λ and C). For this reason, in this section we extend the EM-based maximum likelihood algorithm of Dempster et al. [1977] (see also Browne and McNicholas [2015]) and applied by Bianchi et al. [2016] to estimate the parameters of the MNTS distribution. We consider the extension of the EM algorithm proposed by Liu and Rubin [1994], that is the expectation-conditional maximization either (ECME) algorithm.

Let h be the density function of the subordinator defined in equation (2.6), that is the mixing random variable of the normal mean-variance mixture (2.2). Then, as shown in Hu [2005]), the density function of a MNRDTS random variable can be written as

$$f_Y(y; \Theta) = \int_0^\infty f_{Y|S}(y|s; \mu, \theta, \Sigma) h(s; \alpha, \lambda, C) ds, \quad (3.1)$$

where $Y|S \sim N(\mu + \theta S, S\Sigma)$, and Θ is the set of model parameters $(\alpha, \lambda, C, \theta, \mu, \Sigma)$. The integral in equation (3.1) is useful not only in the n -dimensional case, but also in the univariate case, because it allows one to use the characteristic function of the mixing distribution which is simpler to implement from a numerical perspective than the characteristic function of the MNRDTS univariate component in equation (2.12).

Given a set of N observations $\{Y^k = Y_{t_k} - Y_{t_{k-1}}\}_{k=1, \dots, N}$, instead of focusing on the observed log-likelihood $LL(\Theta; Y^1, \dots, Y^N)$, we consider the following log-likelihood function

$$\begin{aligned} LL(\Theta; Y^1, \dots, Y^N, S^1, \dots, S^N) &= \sum_{k=1}^N \log f_{Y,S}(Y^k, S^k; \Theta) \\ &= \sum_{k=1}^N \log f_{Y|S}(Y^k|S^k; \mu, \theta, \Sigma) + \sum_{k=1}^N \log h_S(S^k; \alpha, \lambda, C) \\ &= L_1(\mu, \theta, \Sigma; Y|S) + L_2(\alpha, \lambda, C; S), \end{aligned} \quad (3.2)$$

where $\Theta = \{\alpha, \lambda, C, \theta, \mu, \Sigma\}$ is the set of parameters, $\{S^k = S_{t_k} - S_{t_{k-1}}\}_{k=1, \dots, N}$ the latent mixing variables coming from the representation (2.2).

We implement an iterative procedure consisting of an expectation step (E-step) in which functions of the latent mixing variable S^k (i.e. S^k and S^{k-1}) are replaced by expected values estimated on the basis of observed data and current parameter estimates, and a maximization step (M-step) in which the parameter estimates are updated. Then, instead of maximizing L_2 we maximize the observed log-likelihood obtained from equation (3.1) with respect to α , λ and C with the other parameters kept fixed at the values of the last update. This results in an ECME algorithm.

The apparently more problematic parameters θ and Σ are in the first term of the log-likelihood (i.e. L_1) and their estimates are relatively easy to derive due to the Gaussian form of this term. In the M-step, first we maximize L_1 to find the parameters of the

conditional normal part L_1 . The maximization of L_1 can be performed analytically, as proven in Chapter 2 of Hu [2005]. The estimates of θ , μ and Σ depend on S^k and S^{k-1} that are replaced by the expected values in equation (3.4) computed numerically by means of the conditional density in equation (3.3). This conditional density is function of observed data Y^k and current parameter estimates.

Thus, the following iterative algorithm is implemented to find a MLE based on (3.2).

1. Set $i = 1$ and select a starting value for $\Theta^{(1)}$, that is $\mu^{(1)} \in \mathbb{R}^n$ is the sample mean, $\theta^{(1)} \in \mathbb{R}^n$ is the zero vector, $V \in \mathbb{R}^n \times \mathbb{R}^n$ is the sample variance-covariance matrix.
2. By considering that

$$f_{S|Y^k}(s; Y^k, \Theta) = \frac{f_{Y|S}(Y^k|s; \mu, \theta, \Sigma)h(s; \alpha, \lambda, C)}{f_Y(Y^k; \Theta)}, \quad (3.3)$$

compute the following weights

$$\begin{aligned} \delta_k^{(i)} &= E(S^{k-1}|Y^k, \Theta^{(i)}), \\ \eta_k^{(i)} &= E(S^k|Y^k, \Theta^{(i)}), \end{aligned} \quad (3.4)$$

3. Evaluate the average values

$$\bar{\delta}^{(i)} = \sum_{k=1}^N \delta_k^{(i)}, \quad \bar{\eta}^{(i)} = \sum_{k=1}^N \eta_k^{(i)}.$$

4. Get the estimates

$$\begin{aligned} \theta^{(i+1)} &= \frac{N^{-1} \sum_{k=1}^N \delta_k^{(i)} (\bar{Y} - Y^k)}{\bar{\delta}^{(i)} \bar{\eta}^{(i)} - 1}, \\ \mu^{(i+1)} &= \frac{N^{-1} \sum_{k=1}^N \delta_k^{(i)} Y^k - \theta^{(i+1)}}{\bar{\delta}^{(i)}}, \\ \Psi^{(i+1)} &= \frac{1}{N} \sum_{k=1}^N \delta_k^{(i)} (Y^k - \mu^{(i+1)})(Y^k - \mu^{(i+1)})' - \bar{\eta}^{(i)} \theta^{(i+1)} \theta^{(i+1)'}, \\ \Sigma^{(i+1)} &= \frac{|V|^{1/n} \Psi^{(i+1)}}{|\Psi^{(i+1)}|^{1/n}}. \end{aligned}$$

5. Set

$$\Theta^{(i')} = \{\alpha^{(i)}, \lambda^{(i)}, C^{(i)}, \theta^{(i+1)}, \mu^{(i+1)}, \Sigma^{(i+1)}\}.$$

6. To complete the calculation of $\Theta^{(i+1)}$, find a , λ , and C that maximize the observed log-likelihood function

$$LL(\Theta^{(i+1)}; Y^1, \dots, Y^N) = \sum_{k=1}^N \log f_Y(Y^k; \Theta^{(i+1)}), \quad (3.5)$$

where $\Theta^{(i+1)} = \{\alpha, \lambda, C, \theta^{(i+1)}, \mu^{(i+1)}, \Sigma^{(i+1)}\}$ and $LL(i)$ is the value of the observed log-likelihood function at the point of maximum.

7. If $i < 100$ and $LL(i) - LL(i - 1) > 0.01$, increment iteration count i and go to step 2, otherwise, stop the algorithm.

While point 2 represents the E-step, points from 4 to 6 describe the M-step. The algorithm converges to the maximum likelihood estimate because the observed log-likelihood is continually increased (see Liu and Rubin [1994]). We set the maximum number of iterations i equal to 100. However, if the following inequality $LL(i) - LL(i - 1) \leq 0.01$ is satisfied, we stop the algorithm. We point out that in the empirical exercise we conduct in this work the algorithm converges after a few iterations, usually less than 10.

The last equality in Step 4 is needed to constrain the determinant of Σ to be the determinant of the sample variance-covariance matrix V . While the starting values of the conditional normal part are defined in Step 1, we select $\alpha = 0.75$, and $\lambda = C = 1$ as starting values for the parameters of the subordinator. These values show a good performance in the practical application we are interested in.

Because it is not possible to find a closed-form solution for f_Y and h , to evaluate these two functions numerical methods based on the characteristic function of the subordinator must be employed. The characteristic function of the RDTS subordinator is given in equation (2.6) and a discrete evaluation of the density function h together with an interpolation algorithm is used to evaluate f_Y . More in details, the fast Fourier transform (FFT) procedure applied to the characteristic function (2.6) allows one to evaluate the density function h , as described by Stoyanov and Racheva-Iotova [2004]. Thus, given a discrete evaluation of the function h , the density f_Y in equation (3.1) is obtained by numerical integration. As described in Section 3.2.2, the same approach can be implemented to evaluate the density function of the j -th marginal distribution in equation (2.12).

Since closed-form solutions are not available, the expectations in equation (3.4) and the ratio in equation (3.3) are also evaluated through numerical integration algorithms. While $f_{Y|S}$ in equation (3.3) can be written in closed-form, since $Y|S^k \sim N(\mu + \theta S^k, S^k \Sigma)$ (see Hu [2005]), the density h is computed by means of a FFT procedure, and the denominator which is the density function given in equation (3.1) is evaluated by numerical integration.

3.2 Evaluating the function G

The evaluation of the characteristic function in equation (2.6) is connected with the function G involving the confluent hypergeometric (or Kummer) function M defined in equation (2.8) and with the confluent hypergeometric function U (see Beals and Wong [2010]). These functions belong to the special function class and often occur in many practical computational problems. Except for specific situations, computing confluent hypergeometric functions is difficult in practice (see Pearson et al. [2017]). The numerical reliability and the efficiency of a computational method implemented to evaluate these functions depends on the parameters and on the variable regimes. It should be noted that for any characteristic function the following equality holds

$$\Psi(-u) = \overline{\Psi(u)}, \quad (3.6)$$

where \bar{z} means the complex conjugate of z . As explained in Section 3.2.1, we consider equation (3.6) to halve the computational burden of the characteristic function evaluation.

3.2.1 The RDTS case

In the applications involving only the RDTS random variable or the RDTS subordinator one does not need a general algorithm to evaluate the function G on the entire complex plane \mathbb{C} , but just on a subset of it, that is on the straight line represented by the subset $I = \{iy \mid y \in \mathbb{R}\}$ of the complex plane \mathbb{C} (see Bianchi et al. [2019]).

In this particular case there is an x^2 as argument of the function M in equation (2.7) and an efficient algorithm to evaluate the characteristic function in equation (2.6) can be constructed. It is not difficult to see in equation (2.6) that if one evaluates the function G on I , the function M is evaluated only on the real line. Equation (3.6) allows us to evaluate the function $\Psi(\cdot)$ only on the negative part of the real line and we obtain the evaluation on the positive part of the real line simply by conjugating. This allows us to determine the values of $G(x; \alpha, \lambda)$ only for the subset $I_- = \{iy \mid y \in \mathbb{R}_-\}$ and then to simply consider the conjugate for the set $I_+ = \{iy \mid y \in \mathbb{R}_+\}$.

For the Kummer function M in equation (2.8) the following equalities hold

$$\begin{aligned} M(a, b; z) &= e^z M(b - a, b; -z), \\ M(a, b; z) &= \frac{\Gamma(b)}{\Gamma(b - a)} (-z)^{-a} \sum_{n=0}^{\infty} (-1)^n \frac{(a)_n (a - b + 1)_n}{z^n n!} \\ &\quad + \cos \pi(b - a) \frac{\Gamma(b)}{\Gamma(a)} \exp(z) z^{a-b} \sum_{n=0}^{\infty} \frac{(b - a)_n (1 - a)_n}{z^n n!}. \end{aligned} \quad (3.7)$$

Thus, in order to obtain a fast convergence of the series (2.10), we split the negative imaginary line I and the negative real line R into two subsets without intersection,

$$\begin{aligned} I_-^1 &= \{iy \mid -30 < y \leq 0\}, \\ I_-^2 &= \{iy \mid y < -30\}, \end{aligned}$$

and

$$\begin{aligned} R_-^1 &= \{y \mid -30 < y \leq 0\}, \\ R_-^2 &= \{y \mid y < -30\}. \end{aligned}$$

Then we use the first equality in (3.7) and (2.8) to evaluate G in I_-^1 (i.e. M in R_-^1). The second equality of (3.7) is enough to evaluate G in I_-^2 (i.e. M in R_-^2). This subdivision allows one to truncate the series (2.8) to the integer $N = 1000$ and obtain the same results as other algorithm implemented in ad-hoc R or Python libraries to evaluate special functions. This method increase considerably the speed with respect to algorithms available in commonly used R or Python libraries, since it is grounded only on basic summations and multiplication.

The evaluation through the FFT algorithm of the density function of the RDTS subordinator ($\alpha = 0.75$ and both λ and C equal to 1) on 10,000 equally spaced points in the interval between 0 and 10 while is almost instantaneous with the ad-hoc algorithm described above, it takes around 50 seconds with a parallel code written in R and calling the Python *mpmath* library. This Python library implements a huge number of special functions, with arbitrary precision and full support for complex numbers. The R *reticulate*

package provides an R interface to Python modules, classes, and functions, allowing one to call user-defined Python functions in an R script. The code is run on a Linux desktop with an AMD FX-6300 processor with 16 GB of RAM (R 4.1.2 and Python 3.8.12). The parallelization is obtained with the *foreach* and *doParallel* libraries of R. Even if with a modern processor the computing time of this second approach can be much lower than 50 seconds, it does not become instantaneous as the ad-hoc algorithm.

3.2.2 The MNRDTS case

The algorithm described in Section 3.2.1 cannot be considered for the evaluation of the characteristic functions of a MNRDTS random variable in equations (2.11) and (2.12). To compute these characteristic functions it is necessary to implement an efficient algorithm for the evaluation of the function M or U on the whole complex plane. In this more general case, the arguments of the function G have non zero real and imaginary parts. The representation of the function G in equation (2.9) involving only a single Kummer U function instead of two different Kummer M functions simplifies the numerical evaluation of the MNRDTS characteristic function.

The series in equation (2.8) together with the equality (2.7) generates numerical errors when the real part of the argument of the function G increases. Additionally, even if the Kummer M converges on the whole complex plane, its value increases exponentially creating instability and cancellation issues (depending on the value of the argument, the function G is the difference between two Kummer M functions). In this more general case we are not able to find a smart solution as in the RDTS case.

It should be noted that there are two alternative approaches to evaluate the density of the j -th marginal distribution of a MNRDTS random variable: (1) it is possible to consider the integral in equation (3.1) and relying on the algorithm described in Section 3.2.1 for the characteristic function of the RDTS subordinator needed to obtain the density h by means of the FFT procedure; (2) it is possible to apply the FFT procedure by directly evaluating the characteristic function of the j -th marginal distribution in equation (2.12).

As in Section 3.2.1, to evaluate the characteristic function (2.12), we consider the Kummer U function implemented in the Python *mpmath* library and equation (3.6) to halve the computational burden of the characteristic function evaluation. This approach is fast enough to be used in practical applications to finance. Furthermore, the evaluation of the Kummer U function on a vector can be easily parallelized to speed up the R code (e.g. with the *foreach* and *doParallel* libraries of R) or the Python code (e.g. with the *multiprocessing* library of Python).

4 Empirical analysis

The analysis is performed on Refinitiv daily dividend-adjusted closing prices from December 31, 2014 through December 31, 2021 for five stock indexes: the Deutsche Aktienindex 30 (ticker DAX), the Cotation Assistée en Continu 40 (ticker CAC), the Financial Times Stock Exchange Milano Indice di Borsa (ticker FTSEMIB), Índice Bursátil Español (ticker IBEX), Amsterdam Exchange Index (ticker AEX) representing five major European indexes. The time period in this study includes the recent Covid-19 pandemic event. In

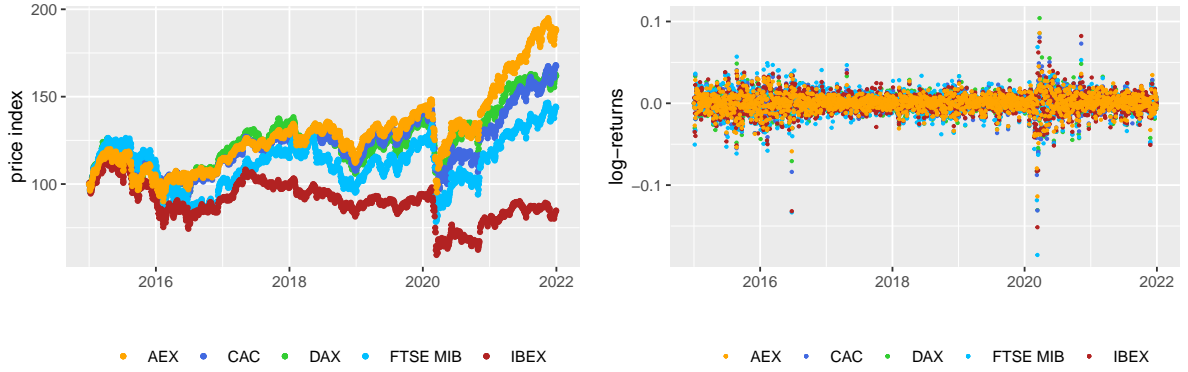


Figure 2: For each index we report the performance and the log-returns from December 31, 2014 to December 31, 2021.

Figure 2 we report the performance of the indexes over the time span considered in this work and the corresponding log-returns.

We consider the constant condition correlation (CCC) model described in McNeil et al. [2005] (see also Paoletta et al. [2021]). After having estimated the volatility model we define the devolatilized process and on this process we estimate the proposed multivariate model. Model estimation is divided into two steps. In the first step, we estimate a univariate AR-GARCH model on the time series of log returns. In the second step, we estimate on the 5-dimensional filtered innovations (or devolatilized) data the dependence structure by applying different multivariate approaches: the multivariate normal to which we refer to as *MNormal*, the MGH, the MNTS and the MNRDTS model. As in Bianchi et al. [2016], from the continuous time Y_t model defined in Section 2, it is straightforward to define the corresponding multivariate random variable, that is the distribution of the increments defined for each discrete-time step Δt . With an abuse of notation, we refer to the discrete time-series of index log-return as y_t .

For each index log-return time-series y_t we assume an AR(1)-GARCH(1,1) model with Glosten-Jagannathan-Runkle (GJR) dynamics for the volatility (see Glosten et al. [1993]), that is

$$\begin{aligned} y_t &= ay_{t-1} + \sigma_t \varepsilon_t + c \\ \sigma_t^2 &= \xi_0 + \xi_1 (|\sigma_{t-1} \varepsilon_{t-1}| - \gamma (\sigma_{t-1} \varepsilon_{t-1}))^2 + \eta_1 \sigma_{t-1}^2, \end{aligned} \quad (4.1)$$

where ε_t is are temporally independent and identically distributed random variables with zero mean and unit variance. Additionally, at each estimation step we test if the autoregressive component is statistically significant: if it is not, we estimate the model without the autoregressive component.

We perform the empirical analysis on 515 rolling windows (between December 31, 2019 and December 31, 2021 there are 515 trading days). Each rolling window has a 5-year length (1,278 trading days): the first window has as starting point December 31, 2014 and ending point December 31, 2019. To assess the extent to which the estimates and the goodness-of-fit vary over time, we repeat the same empirical study on each window. Since we estimate the parameters of each multivariate non-normal model for a total of 515 rolling-window periods, the overall computing time is considerable in both the MNTS and

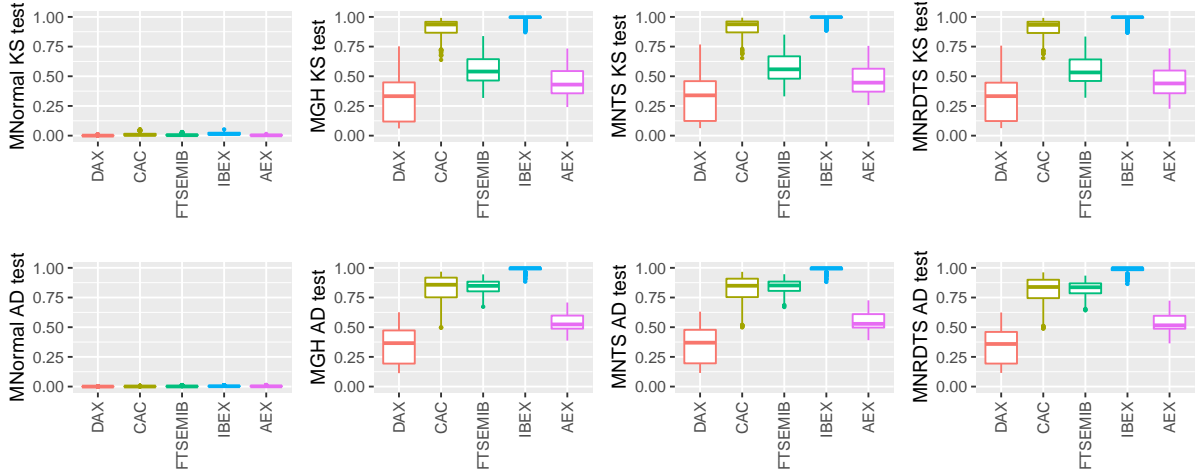


Figure 3: For each index and each model we report the boxplot of the p -value of the KS and the AD tests from December 31, 2019 to December 31, 2021.

the MNRDTS case, even if the MNTS algorithm is two times faster than the MNRDTS one. To deal with this issue we rely on an efficient R code making use of the packages *foreach* and *doParallel* and run it on a multi-core Linux based system and we use all available cores contemporaneously.

For the assessment of the goodness-of-fit, for each margin of our multivariate distributions (i.e. each index ε_t) we conduct the Kolmogorov-Smirnov (KS) and the Anderson-Darling (AD) test over the entire estimation window from December 31, 2019 to December 31, 2021 for a total of 2,575 KS and AD tests for each model (515 for each index). In Figure 3 the p -values of the tests are reported. As far as the KS test is concerned, while the normal model is almost always rejected, for non-normal models the null hypothesis is never rejected. We consider a significance level equal to 0.05. There are not remarkable differences in term of KS and AD statistics between the three non-normal models: the test statistics are almost indistinguishable (see Figure 4). The KS (AD) statistic is on average 0.0202 (0.5702) for the MGH model, 0.0199 (0.5674) for the MNTS model, and 0.0202 (0.5810) for the MNRDTS model. The KS (AD) statistic is larger for the MNormal model, i.e. it is equal to 0.0505 (6.104).

In Figure 5 we show the time-series of the parameters of the mixing random variable of the three normal mean-variance mixture models estimated from December 31, 2019 to December 31, 2021: λ , ψ and χ in the MGH case, α , λ e C in the MNTS and the MNRDTS case. Even if much of the stock market volatility is captured by the discrete-time volatility model in equation (4.1), the estimated parameters of the mixing random variable vary over time. This empirical finding suggests that this additional source of randomness could be captured by assuming a time-varying parameters approach as recently proposed by Kim et al. [2022]. With the exception of a few outliers around June 2021, we observe smooth dynamics for these estimates even during the market turmoil in March 2020. The dynamics of the α estimates of the two tempered stable models slightly differs and this difference is reflected also in the dynamics of λ and C estimates. Nevertheless, on the basis of the values of the AD statistics in Figures 3 and 4, there are not remarkable

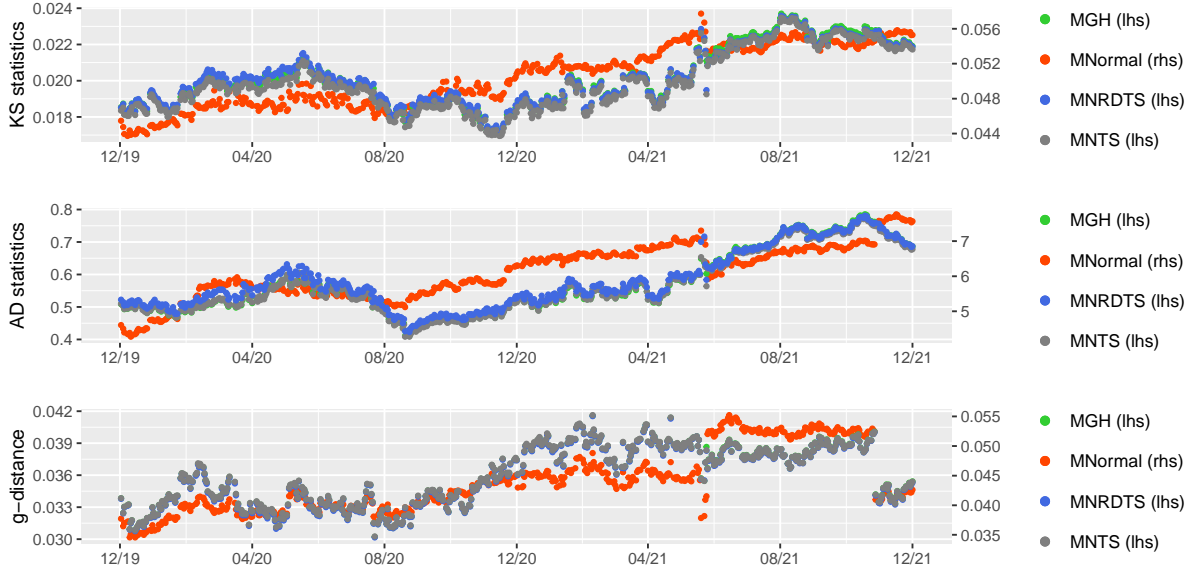


Figure 4: We report for each model the average KS and AD statistics and the g -distance over the five indexes from December 31, 2019 to December 31, 2021. For the MNormal model the values of the statistics are reported on the right side.

differences in the tail behavior of the three non-normal models.

Additionally, we evaluate the average distance between the empirical and theoretical characteristic function and we refer to it as g -distance. For a given grid $u_j \in \mathbb{R}^n$, with j from 1 to q , g is defined as

$$g(\Theta, Y, u_j) = e^{i\langle u_j, Y \rangle} - \Psi_{Y, \Theta}(u_j),$$

where $\langle \cdot, \cdot \rangle$ is the scalar product and the distance is the norm of the vector

$$\bar{g}_{T,j}(\Theta) = \frac{1}{T} \sum_{k=1}^T \left(e^{i\langle u_j, Y^k \rangle} - \Psi_{Y^k, \Theta}(u_j) \right). \quad (4.2)$$

It is evident that the choice of the grid is crucial. For the first dimension we consider a vector of q equally spaced points in the interval between minimum and maximum observed returns. Then, after having fixed a seed, to obtain the vector representing the second dimension, we randomly permute the vector obtained for the first dimension. The same approach is considered for all other dimensions up to five. The value of q is set equal to 50. In Figure 4 we report the time-series of the g -distance from December 31, 2019 to December 31, 2021: it is on average 0.0359 for the MGH model, 0.0359 for the MNTS model, and 0.0358 for the MNRDTS model. It is larger for the MNormal model (0.0439).

Next, as proposed in Xia and Grabchak [2022], we test all components together, using the nonparametric test for equality of densities, which was introduced in Li et al. [2009] and is implemented in the *npdeneqtest* function of the R package *np*. The test statistic is based on the integrated squared difference between two densities and it is evaluated by considering the kernel estimates of these densities (see Li et al. [2009]). We test if this

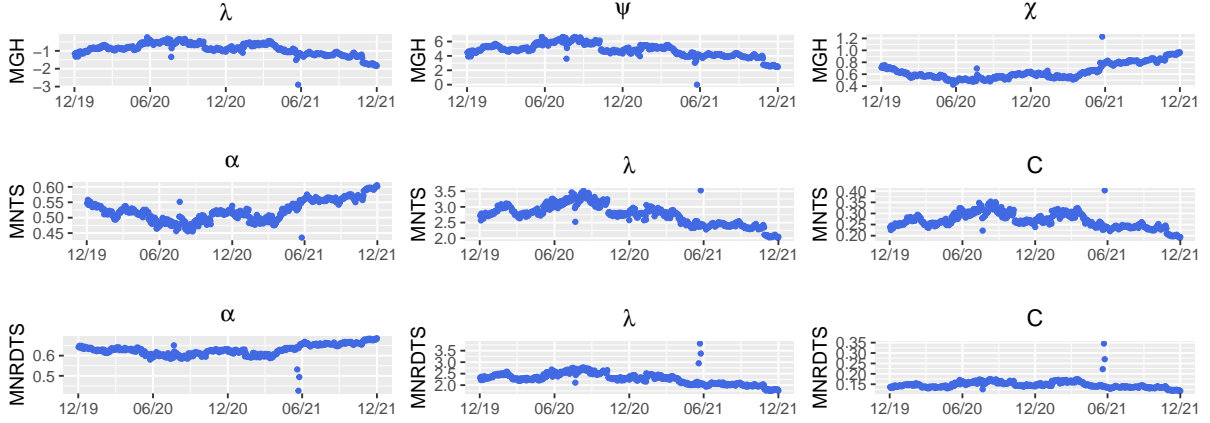


Figure 5: We report the time-series of the estimates of the parameters of the mixing random variable of the three multivariate normal mean-variance mixture models in the time span from December 31, 2019 to December 31, 2021.

estimated distance between observed and simulated data is significantly different from zero. As the computing time of the test is around 25 minutes for each model, we conduct it only on the last estimation date. For each model, we compare the 5-dimensional filtered market data to the simulated samples based on estimated parameters. The number of observations of the simulated sample is the same of the observed one (i.e. 1,278 trading days). While the null hypothesis of equality is rejected in the MNormal case, in all non-normal cases is not possible to reject it at the 10% tail probability level. The p -value of the test is 0 for MNormal model, 0.81 for the MGH model, 0.60 for the MNTS model and 0.78 for the MNRDTS model. It should be noted that the stochastic representation in equation (2.2) allows one to simulate random variates from these non-normal models by drawing random samples from the multivariate normal and the mixing random variable. While in the MGH the simulation of the mixing random variable is obtained through the *rgig* function of the *ghyp* package of R, the simulation of CTS and RDTS random draws is not a simple task and an ad-hoc implementation is needed (see Bianchi et al. [2017] for a detailed description).

The margins of the MNormal model are normally distributed and they do not assign enough weight to tail events and are not able of explaining negative skewness. A visual assessment of these empirically observed facts is provided in Figure 6 where we show the simulated innovations drawn from a MNormal (MNRDTS) model fitted on filtered market data and compare them to observed filtered market data. The number of simulations is equal to the number of observed market data.

5 A simulation study

After having conducted in Section 4 an extensive empirical analysis of the MNRDTS model on the time-series of observed log-returns, we empirically study through a simulation exercise the estimation algorithm presented in Section 3.1. A similar exercise

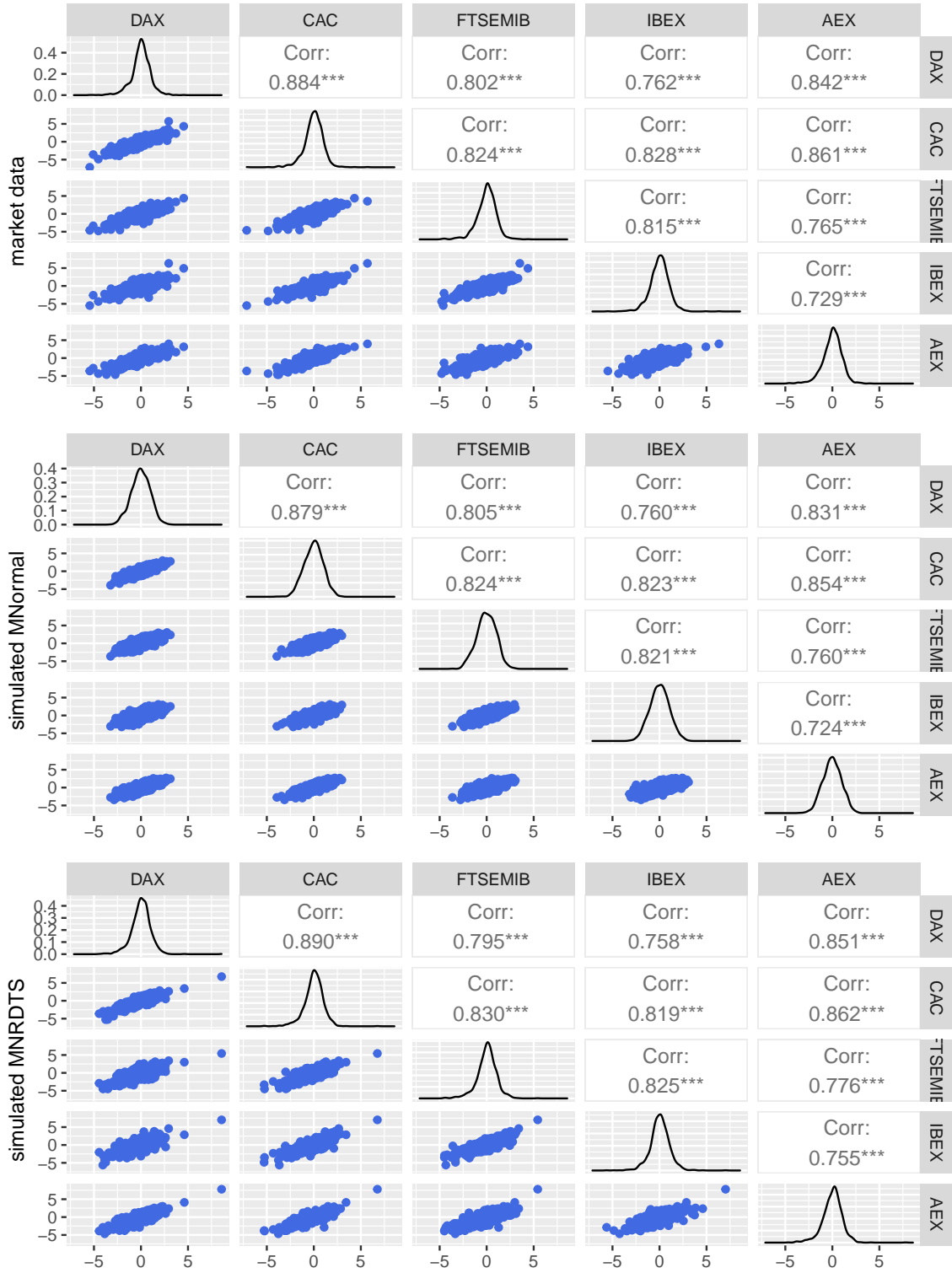


Figure 6: Bivariate scatterplots of filtered market data and simulated innovations from the MNormal and the MNRDTS. Depicted market data are daily log-returns from December 31, 2017 to December, 31 2021.

	α	λ	C	μ	θ	Σ
MSE	0.029	0.576	0.041	[0.053, 0.055]	[0.194, 0.208]	[0.218, 0.265]
ARPE	0.060	0.215	0.226	[0.161, 0.212]	[0.191, 0.254]	[0.067, 0.076]
RE ^{0.9}	0.115	0.411	0.480	[0.253, 0.337]	[0.329, 0.419]	[0.115, 0.4725]

Table 1: Errors between true parameters and estimates of a MNRDTS distribution. Mean square error (MSE), root mean square error (RMSE), and relative error (RE). For the parameters μ , θ and Σ we report the range of variation of the errors.

conducted on the MNTS model is described in Bianchi et al. [2016]. More specifically, we generate MNRDTS random numbers by considering the set of parameters estimated on the devolatilized time-series of the main European stock indexes from December 31, 2016 through December 31, 2021 (see Section 4), and then we estimate the parameter by following the extension of the EM algorithm defined in Section 3.1. To simulate the univariate RDTS mixing distribution we consider the inverse transform algorithm described by Bianchi et al. [2017]. We repeat the exercise 1,000 times by considering samples with 1,278 observations (i.e. the number of trading days between December 31, 2016 and December 31, 2021).

Table 1 contains the value of the mean square error (MSE), the average relative percentage error (ARPE), and the relative error (RE) of the parameter estimators. The MSE and the ARPE of the parameter p are defined by

$$MSE(p) = \frac{1}{Nsim} \sum_{i=1}^{Nsim} (p - \hat{p}_i)^2 \quad (5.1)$$

and

$$ARPE(p) = \frac{1}{Nsim} \sum_{i=1}^{Nsim} \left| \frac{p - \hat{p}_i}{p} \right|, \quad (5.2)$$

where $Nsim$ is the number of simulations, which is equal to 1,000, and \hat{p}_i is the estimate of p in the i -th simulated scenario. Finally, the RE of the parameter p is defined by

$$RE^{1-\delta}(p) = \max \left\{ \left| \frac{p - q_{\delta/2}(\hat{p})}{p} \right|, \left| \frac{p - q_{1-\delta/2}(\hat{p})}{p} \right| \right\}, \quad (5.3)$$

where $q_{\beta}(\hat{p})$ represents the β -th quantile of the empirical distribution of \hat{p} . We select δ equal to 0.2. It should be noted that by following the same approach it is possible to obtain the standard errors of the estimates.

In Figure 7 we show the violin plot of the empirical distribution of the relative difference between the true values and the estimated parameters. The relative difference is defined by the ratio of $p - \hat{p}_i$ to p , where i range from 1 to $Nsim$. We observe that medians (the central mark) are close to zero, that is the estimated parameters are close to the corresponding true values. Based on the errors reported in Table 1, the accuracy of the estimator α is higher than the one for C and λ , and the one for Σ is higher than the one for μ and θ . The errors of C , λ , μ , and θ are generally high. Similar results were observed in the MNTS case (see Bianchi et al. [2016]). This may be caused by the large number of model parameters and the relative small number of simulations. As shown in

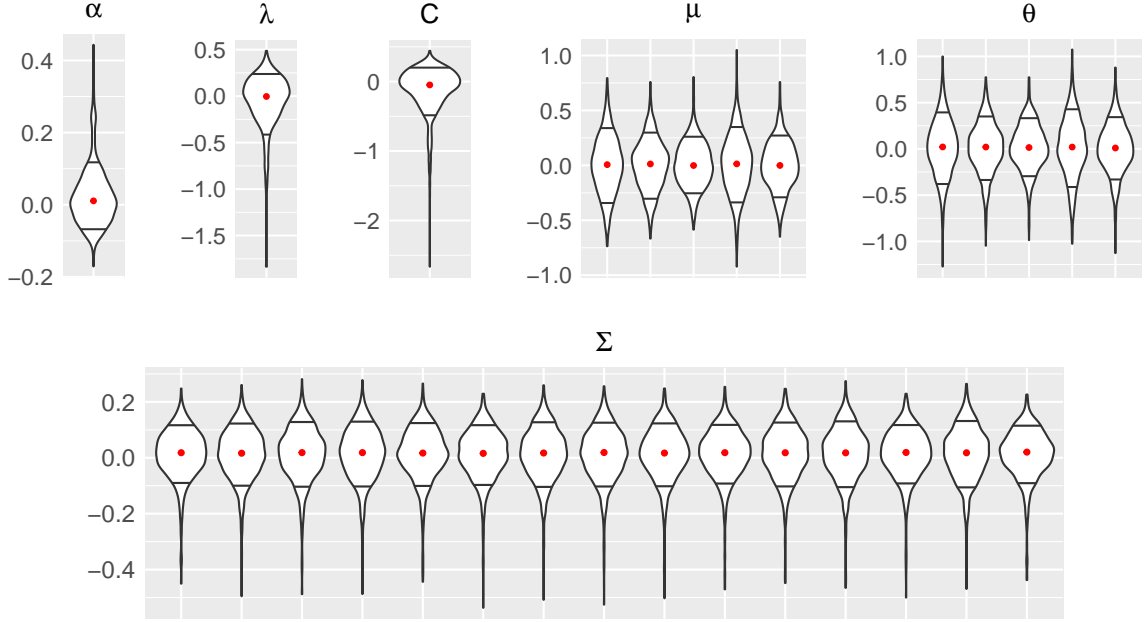


Figure 7: Violin plots of the relative difference between true parameters and estimates of a MNRDTS distribution. Each plot consists of 1,000 estimates. MNRDTS random numbers are generated by considering the set parameters estimated on the time-series with 1,278 log-return observations ending on December 31, 2021. While the central mark represents the median value, the horizontal upper (lower) line identifies the 0.9 (0.1) quantile. For the matrix Σ we report only the diagonal and the lower diagonal values.

Bianchi et al. [2017] for tempered stable models, a large number of simulations is needed to obtain small errors. We also conducted the same exercise on a multivariate normal distribution. In particular, the accuracy of the correlation $\hat{\Sigma}$ in the normal case is only slightly better than that of the $\hat{\Sigma}$ in the MNRDTS case.

6 Conclusions

In this work, we have focused our attention on the practical implementation of numerical methods involving the use of RDTS random variables in the field of finance. Basic definitions and formulas are given and possible algorithms to evaluate the characteristic function of a MNRDTS random variable and its density function are discussed. Furthermore, an empirical analysis on a five-dimensional time series of index log-returns is conducted to compare the MNRDTS model with possible competitor multivariate models.

References

- M. Abramowitz and I. Stegun. *Handbook of mathematical functions with formulas, graphs, and mathematical tables*. Dover Publications, New York, 1974.
- R. Beals and R. Wong. *Special functions: a graduate text*. Cambridge University Press, Cambridge, UK, 2010.
- M.L. Bianchi. Are the log-returns of Italian open-end mutual funds normally distributed? A risk assessment perspective. *Journal of Asset Management*, 16(7):437–449, 2015.
- M.L. Bianchi, S.T. Rachev, Y.S. Kim, and F.J. Fabozzi. Tempered infinitely divisible distributions and processes. *Theory of Probability & Its Applications*, 55(1):2–26, 2011.
- M.L. Bianchi, G.L. Tassinari, and F.J. Fabozzi. Riding with the four horsemen and the multivariate normal tempered stable model. *International Journal of Theoretical and Applied Finance*, 19(4), 2016.
- M.L. Bianchi, S.T. Rachev, and F.J. Fabozzi. Tempered stable Ornstein-Uhlenbeck processes: A practical view. *Communications in Statistics - Simulation and Computation*, 423-445(1):59–86, 2017.
- M.L. Bianchi, S.V. Stoyanov, G.L. Tassinari, F.J. Fabozzi, and S.M. Focardi. *Handbook of heavy-tailed distributions in asset management and risk management*. World Scientific, 2019.
- M.L. Bianchi, A. Hitaj, and G.L. Tassinari. A welcome to the jungle of multivariate non-Gaussian models applied to finance. *Annals of Operations Research*, 2022.
- S.A. Broda and J.A. Zambrano. On quadratic forms in multivariate generalized hyperbolic random vectors. *Biometrika*, 108(2):413–424, 2021.
- R.P. Browne and P.D. McNicholas. A mixture of generalized hyperbolic distributions. *Canadian Journal of Statistics*, 43(2):176–198, 2015.
- B. Buchmann, B. Kaehler, R. Maller, and A. Szimayer. Multivariate subordination using generalised Gamma convolutions with applications to Variance Gamma processes and option pricing. *Stochastic Processes and their Applications*, 127(7):2208–2242, 2017.
- A.P. Dempster, N.M. Laird, and D.B. Rubin. Maximum likelihood from incomplete data via the EM algorithm. *Journal of the Royal Statistical Society: Series B*, 39(1):1–22, 1977.
- H.A. Fallahgoul and G. Loeper. Modelling tail risk with tempered stable distributions: an overview. *Annals of Operations Research*, 299:1253–1280, 2021.
- H.A. Fallahgoul, Y.S. Kim, F.J. Fabozzi, and J. Park. Quanto option pricing with Lévy models. *Computational Economics*, 53(3):1279–1308, 2019.
- H.A. Fallahgoul, J. Hugonnier, and L. Mancini. Risk Premia and Lévy Jumps: Theory and Evidence. *Journal of Financial Econometrics*, 2021.

- L.R. Glosten, R. Jagannathan, and R.E. Runkle. On the relation between the expected value and the volatility of the nominal excess return on stocks. *Journal of Finance*, 48(5):1779–1801, 1993.
- M. Grabchak. *Tempered stable distributions: Stochastic models for multiscale processes*. Springer, Cham, 2016.
- M. Grabchak. An exact method for simulating rapidly decreasing tempered stable distributions in the finite variation case. *Statistics & Probability Letters*, 170:109015, 2021.
- W. Hu. *Calibration of multivariate generalized hyperbolic distributions using the EM algorithm, with applications in risk management, portfolio optimization and portfolio credit risk*. PhD thesis, Florida State University, 2005.
- Y. S. Kim, D. Jiang, and S. Stoyanov. Long and short memory in the risk-neutral pricing process. *The Journal of Derivatives*, 26(4):71–88, 2019.
- Y.S. Kim, S.T. Rachev, M.L. Bianchi, and F.J. Fabozzi. Tempered stable and tempered infinitely divisible GARCH models. *Journal of Banking and Finance*, 34(9):2096–2109, 2010.
- Y.S. Kim, K.H. Roh, and R. Douady. Tempered stable processes with time-varying exponential tails. *Quantitative Finance*, 22(3):541–561, 2022.
- Q. Li, E. Maasoumi, and J.S. Racine. A nonparametric test for equality of distributions with mixed categorical and continuous data. *Journal of Econometrics*, 148(2):186–200, 2009.
- C. Liu and D.B. Rubin. The ECME algorithm: A simple extension of EM and ECM with faster monotone convergence. *Biometrika*, 81(4):633–648, 1994.
- E. Luciano and P. Semeraro. Multivariate time changes for Lévy asset models: Characterization and calibration. *Journal of Computational and Applied Mathematics*, 233(8):1937–1953, 2010.
- A. McNeil, R. Frey, and P. Embrechts. *Quantitative risk management: Concepts, techniques, and tools*. Princeton University Press, 2005.
- M.S. Paolella, P. Polak, and P.S. Walker. A non-elliptical orthogonal GARCH model for portfolio selection under transaction costs. *Journal of Banking & Finance*, 125:106046, 2021.
- J.W. Pearson, S. Olver, and M.A. Porter. Numerical methods for the computation of the confluent and Gauss hypergeometric functions. *Numerical Algorithms*, 74(3):821–866, 2017.
- R.S. Protasov. EM-based maximum likelihood parameter estimation for multivariate generalized hyperbolic distributions with fixed λ . *Statistics and Computing*, 14(1):67–77, 2004.

- J. Rosinski. Tempering stable processes. *Stochastic processes and their applications*, 117(6):677–707, 2007.
- S. Stoyanov and B. Racheva-Iotova. Numerical methods for stable modeling in financial risk management. In S.T. Rachev, editor, *Handbook of computational and numerical methods in finance*, pages 299–329. Birkhäuser, 2004.
- Y. Xia and M. Grabchak. Estimation and simulation for multivariate tempered stable distributions. *Journal of Statistical Computation and Simulation*, 92(3):451–475, 2022.

A Appendix

A.1 RTDS subordinator moments

A process $S = \{S_t, t \geq 0\}$ with Lévy measure given by

$$\nu(dx) = C \frac{e^{-\frac{\lambda^2 x^2}{2}}}{x^{\alpha+1}} I_{x>0} dx, \quad (\text{A.1})$$

where $\lambda > 0$, $C > 0$, $0 < \alpha < 1$ and Lévy triplet $(0, \nu, 0)$ is said to be a RDTS subordinator. The characteristic function of S_t is given by

$$\Psi_{S_t}(u) = E[\exp(iuS_t)] = \exp(tl(iu)) = \exp \left[t \int_0^{+\infty} (e^{iux} - 1) C \frac{e^{-\frac{\lambda^2 x^2}{2}}}{x^{\alpha+1}} dx \right]. \quad (\text{A.2})$$

To simplify, we set $s = iu$ and the characteristic function can be obtained by evaluating the integral (see also Bianchi et al. [2011] and the online Appendix of Fallahgoul et al. [2019])

$$\begin{aligned} \int_0^{+\infty} (e^{sx} - 1) C \frac{e^{-\frac{\lambda^2 x^2}{2}}}{x^{\alpha+1}} dx &= C \int_0^{+\infty} \left(\sum_{k=0}^{+\infty} \frac{(sx)^k}{k!} - 1 \right) \frac{e^{-\frac{\lambda^2 x^2}{2}}}{x^{\alpha+1}} dx \\ &= C \int_0^{+\infty} \sum_{k=1}^{+\infty} \frac{(sx)^k}{k!} \frac{e^{-\frac{\lambda^2 x^2}{2}}}{x^{\alpha+1}} dx \\ &= C \sum_{k=1}^{+\infty} \frac{(sx)^k}{k!} \int_0^{+\infty} \frac{e^{-\frac{\lambda^2 x^2}{2}}}{x^{\alpha+1}} dx \\ &= C \sum_{k=1}^{+\infty} \frac{s^k}{k!} \int_0^{+\infty} x^k \frac{e^{-\frac{\lambda^2 x^2}{2}}}{x^{\alpha+1}} dx \\ &= C \sum_{k=1}^{+\infty} \frac{s^k}{k!} \left(\frac{1}{2} \left(\frac{2}{\lambda^2} \right)^{\frac{k-\alpha}{2}} \Gamma\left(\frac{k-\alpha}{2}\right) \right) \\ &= \frac{C}{2} \sum_{k=1}^{+\infty} \frac{s^k}{k!} \left(\frac{2}{\lambda^2} \right)^{\frac{k-\alpha}{2}} \Gamma\left(\frac{k-\alpha}{2}\right) \\ &= \frac{C}{2} \sum_{k=1}^{+\infty} \frac{s^k}{k!} \left(\frac{2}{\lambda^2} \right)^{\frac{k}{2}} \left(\frac{2}{\lambda^2} \right)^{-\frac{\alpha}{2}} \Gamma\left(\frac{k-\alpha}{2}\right) \\ &= \frac{C}{2} \sum_{k=1}^{+\infty} \frac{s^k}{k!} \left(\frac{\sqrt{2}}{\lambda} \right)^k \left(\frac{\sqrt{2}}{\lambda} \right)^{-\alpha} \Gamma\left(\frac{k-\alpha}{2}\right) \\ &= \frac{C}{2} \left(\frac{\lambda}{\sqrt{2}} \right)^{\alpha} \sum_{k=1}^{+\infty} \frac{s^k}{k!} \left(\frac{\sqrt{2}}{\lambda} \right)^k \Gamma\left(\frac{k-\alpha}{2}\right) \end{aligned}$$

$$= C \frac{\lambda^\alpha}{2^{\frac{\alpha}{2}+1}} \sum_{k=1}^{+\infty} \frac{1}{k!} \left(\frac{\sqrt{2}}{\lambda} s \right)^k \Gamma\left(\frac{k-\alpha}{2}\right).$$

The infinite sum

$$C \frac{\lambda^\alpha}{2^{\frac{\alpha}{2}+1}} \sum_{k=1}^{+\infty} \frac{1}{k!} \left(\frac{\sqrt{2}}{\lambda} s \right)^k \Gamma\left(\frac{k-\alpha}{2}\right) \quad (\text{A.3})$$

has to be split into the infinite sum of even and that of odd terms. The sum of even terms can be written as

$$\begin{aligned} & \sum_{n=1}^{+\infty} \frac{1}{2n!} \left(\frac{\sqrt{2}}{\lambda} s \right)^{2n} \Gamma\left(\frac{2n-\alpha}{2}\right) \\ &= \sum_{n=1}^{+\infty} \frac{1}{\Gamma(2n+1)} \left(\frac{\sqrt{2}}{\lambda} s \right)^{2n} \Gamma\left(n - \frac{\alpha}{2}\right) \\ &= \sum_{n=1}^{+\infty} \frac{1}{2n\Gamma(2n)} \left(\frac{\sqrt{2}}{\lambda} s \right)^{2n} \Gamma\left(n - \frac{\alpha}{2}\right) \\ &= \sum_{n=1}^{+\infty} \frac{\Gamma(\frac{1}{2})}{2n\Gamma(n)\Gamma(n + \frac{1}{2})2^{2n-1}} \left(\frac{\sqrt{2}}{\lambda} s \right)^{2n} \Gamma\left(n - \frac{\alpha}{2}\right) \\ &= \sum_{n=1}^{+\infty} \frac{\Gamma(\frac{1}{2})}{2n\Gamma(n)\Gamma(n + \frac{1}{2})2^{2n-1}} \left(\frac{2}{\lambda^2} s^2 \right)^n \Gamma\left(n - \frac{\alpha}{2}\right) \\ &= \sum_{n=1}^{+\infty} \frac{\Gamma(\frac{1}{2})}{2^{2n}n\Gamma(n)\Gamma(n + \frac{1}{2})} \left(\frac{2}{\lambda^2} s^2 \right)^n \Gamma\left(n - \frac{\alpha}{2}\right) \\ &= \sum_{n=1}^{+\infty} \frac{\Gamma(\frac{1}{2})}{4^n n! \Gamma(n + \frac{1}{2})} \left(\frac{2}{\lambda^2} s^2 \right)^n \Gamma\left(n - \frac{\alpha}{2}\right) \\ &= \Gamma\left(-\frac{\alpha}{2}\right) \sum_{n=1}^{+\infty} \frac{1}{n!} \left(\frac{1}{2\lambda^2} s^2 \right)^n \frac{\Gamma(n - \frac{\alpha}{2})\Gamma(\frac{1}{2})}{\Gamma(-\frac{\alpha}{2})\Gamma(n + \frac{1}{2})} \\ &= \Gamma\left(-\frac{\alpha}{2}\right) \left[\sum_{n=0}^{+\infty} \frac{1}{n!} \left(\frac{1}{2\lambda^2} s^2 \right)^n \frac{\Gamma(n - \frac{\alpha}{2})\Gamma(\frac{1}{2})}{\Gamma(-\frac{\alpha}{2})\Gamma(n + \frac{1}{2})} - 1 \right] \\ &= \Gamma\left(-\frac{\alpha}{2}\right) \left[M\left(-\frac{\alpha}{2}; \frac{1}{2}; \frac{s^2}{2\lambda^2}\right) - 1 \right]. \end{aligned}$$

The sum of odd terms can be written as

$$\sum_{n=0}^{+\infty} \frac{1}{(2n+1)!} \left(\frac{\sqrt{2}}{\lambda} s \right)^{2n+1} \Gamma\left(\frac{2n+1-\alpha}{2}\right)$$

$$\begin{aligned}
&= \sum_{n=1}^{+\infty} \frac{1}{\Gamma(2(n+1))} \left(\frac{\sqrt{2}}{\lambda} s \right)^{2n+1} \Gamma\left(n + \frac{1-\alpha}{2}\right) \\
&= \frac{\sqrt{2}}{\lambda} s \sum_{n=1}^{+\infty} \frac{\Gamma\left(\frac{1}{2}\right)}{\Gamma(n+1)\Gamma(n+\frac{3}{2})2^{2n+1}} \left(\frac{\sqrt{2}}{\lambda} s \right)^{2n} \Gamma\left(n + \frac{1-\alpha}{2}\right) \\
&= \frac{\sqrt{2}}{2\lambda} s \sum_{n=1}^{+\infty} \frac{\Gamma\left(\frac{1}{2}\right)}{\Gamma(n+1)\Gamma(n+\frac{3}{2})4^n} \left(\frac{2}{\lambda^2} s^2 \right)^n \Gamma\left(n + \frac{1-\alpha}{2}\right) \\
&= \frac{\sqrt{2}}{2\lambda} s \sum_{n=1}^{+\infty} \frac{\Gamma\left(\frac{1}{2}\right)}{n!\Gamma(n+\frac{3}{2})} \left(\frac{1}{2\lambda^2} s^2 \right)^n \Gamma\left(n + \frac{1-\alpha}{2}\right) \\
&= \frac{\sqrt{2}}{2\lambda} \frac{\Gamma\left(\frac{1-\alpha}{2}\right)\Gamma\left(\frac{1}{2}\right)}{\Gamma\left(\frac{3}{2}\right)} s \sum_{n=0}^{+\infty} \frac{1}{n!} \left(\frac{1}{2\lambda^2} s^2 \right)^n \frac{\Gamma\left(\frac{3}{2}\right)\Gamma\left(n + \frac{1-\alpha}{2}\right)}{\Gamma\left(\frac{1-\alpha}{2}\right)\Gamma\left(n + \frac{3}{2}\right)} \\
&= \frac{\sqrt{2}}{2\lambda} \frac{\Gamma\left(\frac{1-\alpha}{2}\right)\Gamma\left(\frac{1}{2}\right)}{\frac{1}{2}\Gamma\left(\frac{1}{2}\right)} s M\left(\frac{1-\alpha}{2}; \frac{3}{2}; \frac{s^2}{2\lambda^2}\right) \\
&= \frac{\sqrt{2}}{\lambda} \Gamma\left(\frac{1-\alpha}{2}\right) M\left(\frac{1-\alpha}{2}; \frac{3}{2}; \frac{s^2}{2\lambda^2}\right) s.
\end{aligned}$$

Combining the previous equations, we get

$$\begin{aligned}
\int_0^{+\infty} (e^{sx} - 1) C \frac{e^{-\frac{\lambda^2 x^2}{2}}}{x^{\alpha+1}} dx &= C \frac{\lambda^\alpha}{2^{\frac{\alpha}{2}+1}} \sum_{k=1}^{+\infty} \frac{1}{k!} \left(\frac{\sqrt{2}}{\lambda} s \right)^k \Gamma\left(\frac{k-\alpha}{2}\right) \\
&= C \frac{\lambda^\alpha}{2^{\frac{\alpha}{2}+1}} \left\{ \Gamma\left(-\frac{\alpha}{2}\right) \left[M\left(-\frac{\alpha}{2}; \frac{1}{2}; \frac{s^2}{2\lambda^2}\right) - 1 \right] \right. \\
&\quad \left. + \frac{\sqrt{2}}{\lambda} \Gamma\left(\frac{1-\alpha}{2}\right) M\left(\frac{1-\alpha}{2}; \frac{3}{2}; \frac{s^2}{2\lambda^2}\right) s \right\}. \tag{A.4}
\end{aligned}$$

Taking into account equations (A.2) and (A.4), and substituting s with iu , we get the characteristic function of S_t

$$\begin{aligned}
\Psi_{S_t}(u) &= \exp \left(t C \frac{\lambda^\alpha}{2^{\frac{\alpha}{2}+1}} \left\{ \Gamma\left(-\frac{\alpha}{2}\right) \left[M\left(-\frac{\alpha}{2}; \frac{1}{2}; \frac{-u^2}{2\lambda^2}\right) - 1 \right] \right. \right. \\
&\quad \left. \left. + \frac{\sqrt{2}}{\lambda} \Gamma\left(\frac{1-\alpha}{2}\right) M\left(\frac{1-\alpha}{2}; \frac{3}{2}; \frac{-u^2}{2\lambda^2}\right) iu \right\} \right).
\end{aligned}$$

Furthermore, defining

$$G(x; \alpha; \lambda) = \sum_{k=1}^{+\infty} \frac{x^k}{k!} \left(\frac{\sqrt{2}}{\lambda} \right)^k \Gamma\left(\frac{k-\alpha}{2}\right), \tag{A.5}$$

we can write the characteristic function as

$$\Psi_{S_t}(u) = E[\exp(iuS_t)] = \exp \left(t 2^{-\frac{\alpha}{2}-1} C \lambda^\alpha G(iu; \alpha, \lambda) \right). \tag{A.6}$$

Then, by using the cumulant characteristic function

$$g_{S_t}(u) = tC \frac{\lambda^\alpha}{2^{\frac{\alpha}{2}+1}} G(iu; \alpha; \lambda), \quad (\text{A.7})$$

one can derive the cumulant of order n as

$$\begin{aligned} c_n[S_t] &= \frac{1}{i^n} \frac{d}{du} g_{S_t}(u)|_{u=0} \\ &= K \frac{1}{i^n} \frac{d}{du} G(iu; \alpha; \lambda)|_{u=0} \\ &= K \left(\frac{\sqrt{2}}{\lambda} \right)^n \Gamma\left(\frac{n-\alpha}{2}\right), \end{aligned} \quad (\text{A.8})$$

where

$$K = tC \frac{\lambda^\alpha}{2^{\frac{\alpha}{2}+1}}.$$

Therefore,

$$\begin{aligned} E[S_t] &= c_1(S_t) = tC \frac{\lambda^\alpha}{2^{\frac{\alpha}{2}+1}} \left(\frac{\sqrt{2}}{\lambda} \right) \Gamma\left(\frac{1-\alpha}{2}\right) = tC \lambda^{\alpha-1} 2^{-\frac{\alpha+1}{2}} \Gamma\left(\frac{1-\alpha}{2}\right), \\ \text{var}[S_t] &= c_2(S_t) = tC \frac{\lambda^\alpha}{2^{\frac{\alpha}{2}+1}} \left(\frac{\sqrt{2}}{\lambda} \right)^2 \Gamma\left(\frac{2-\alpha}{2}\right) = tC \lambda^{\alpha-2} 2^{-\frac{\alpha}{2}} \Gamma\left(1 - \frac{\alpha}{2}\right) \\ \text{skew}[S_t] &= \frac{c_3(S_t)}{c_2(S_t)^{3/2}} = t^{-\frac{1}{2}} C^{-\frac{1}{2}} 2^{\frac{\alpha+2}{4}} \lambda^{-\frac{\alpha}{2}} \Gamma\left(\frac{3-\alpha}{2}\right) \left(\Gamma\left(1 - \frac{\alpha}{2}\right)\right)^{-3/2}, \\ \text{kurt}[S_t] &= 3 + \frac{c_4(S_t)}{c_2(S_t)^2} = 3 + t^{-1} C^{-1} \lambda^{-\alpha} 2^{\frac{\alpha+2}{2}} \Gamma\left(2 - \frac{\alpha}{2}\right) \left(\Gamma\left(1 - \frac{\alpha}{2}\right)\right)^{-2}. \end{aligned}$$

A.2 MNRTDS moments

The Laplace exponent of the RDTs subordinator is

$$l_{S_t}(u) = \ln \phi_{S_t}(-iu) = t 2^{-\frac{\alpha}{2}-1} C \lambda^\alpha G(u; \alpha, \lambda),$$

and by considering equation (2.3) we get the characteristic function of the MNRTDS process with linear drift

$$\Psi_{Y_t}(u) = \exp \left(i t u' \mu + t 2^{-\frac{\alpha}{2}-1} C \lambda^\alpha G \left(i u' \theta - \frac{1}{2} u' \Sigma u; \alpha, \lambda \right) \right). \quad (\text{A.9})$$

Setting $u_i = 0, \forall i \neq j$, into (A.9) we get the characteristic function of the j -th marginal distribution

$$\Psi_{Y_{j,t}}(u_j) = \exp \left(i t u_j \mu_j + t 2^{-\frac{\alpha}{2}-1} C \lambda^\alpha G \left(i u_j \theta_j - \frac{1}{2} u_j^2 \sigma_j^2; \alpha, \lambda \right) \right).$$

From the cumulant characteristic function

$$g_{Y_t}(u) = itu'\mu + t2^{-\frac{\alpha}{2}-1}C\lambda^\alpha G\left(iu'\theta - \frac{1}{2}u'\Sigma u; \alpha, \lambda\right),$$

we can derive the first four cumulants. Therefore,

$$\begin{aligned} c_1(Y_{j,t}) &= \mu_j t + K\theta_j \frac{\sqrt{2}}{\lambda} \Gamma\left(\frac{1-\alpha}{2}\right), \\ c_2(Y_{j,t}) &= K\left(\theta_j^2 \left(\frac{\sqrt{2}}{\lambda}\right)^2 \Gamma\left(\frac{2-\alpha}{2}\right) + \sigma_j^2 \frac{\sqrt{2}}{\lambda} \Gamma\left(\frac{1-\alpha}{2}\right)\right), \\ c_3(Y_{j,t}) &= K\left(\theta_j^3 \left(\frac{\sqrt{2}}{\lambda}\right)^3 \Gamma\left(\frac{3-\alpha}{2}\right) + 3\theta_j \sigma_j^2 \left(\frac{\sqrt{2}}{\lambda}\right)^2 \Gamma\left(\frac{2-\alpha}{2}\right)\right), \\ c_4(Y_{j,t}) &= K\left(\theta_j^4 \left(\frac{\sqrt{2}}{\lambda}\right)^4 \Gamma\left(\frac{4-\alpha}{2}\right) + 6\theta_j^2 \sigma_j^2 \left(\frac{\sqrt{2}}{\lambda}\right)^3 \Gamma\left(\frac{3-\alpha}{2}\right) \right. \\ &\quad \left. + 3\sigma_j^4 \left(\frac{\sqrt{2}}{\lambda}\right)^2 \Gamma\left(\frac{2-\alpha}{2}\right)\right) \end{aligned}$$

and the moments are given by the following formulas

$$\begin{aligned} E[Y_{j,t}] &= c_1(Y_{j,t}), \\ var[Y_{j,t}] &= c_2(Y_{j,t}), \\ skew[Y_{j,t}] &= \frac{c_3(Y_{j,t})}{c_2(Y_{j,t})^{3/2}}, \\ kurt[Y_{j,t}] &= 3 + \frac{c_4(Y_{j,t})}{c_2(Y_{j,t})^2}. \end{aligned}$$

The covariances and the correlations are

$$cov(Y_{j,t}, Y_{k,t}) = K \left(g_2 \theta_j \theta_k \left(\frac{\sqrt{2}}{\lambda}\right)^2 + g_1 \sigma_j \sigma_k \frac{\sqrt{2}}{\lambda} \right), \quad (\text{A.10})$$

$$corr(Y_{j,t}, Y_{k,t}) = \frac{g_2 \sqrt{2} \theta_j \theta_k + g_1 \sigma_j \sigma_k \lambda}{\sqrt{2g_2^2 \theta_j^2 \theta_k^2 + g_1^2 \sigma_j^2 \sigma_k^2 \lambda^2 + \sqrt{2} g_1 g_2 (\theta_j^2 \sigma_k^2 + \theta_k^2 \sigma_j^2) \lambda}}, \quad (\text{A.11})$$

where $g_1 = \Gamma\left(\frac{1-\alpha}{2}\right)$, and $g_2 = \Gamma\left(\frac{2-\alpha}{2}\right)$.

A.3 Function G

In this Section we show how to write the function G in equation (2.7) in terms of the confluent hypergeometric function of second kind. The following equality holds

$$G(x; \alpha, \lambda) = \Gamma\left(-\frac{\alpha}{2}\right) \left(M\left(-\frac{\alpha}{2}, \frac{1}{2}; \frac{x^2}{2\lambda^2}\right) - 1 \right) + \frac{\sqrt{2}x}{\lambda} \Gamma\left(\frac{1-\alpha}{2}\right) M\left(\frac{1-\alpha}{2}, \frac{3}{2}; \frac{x^2}{2\lambda^2}\right),$$

where $M(a, b; z)$ is the Kummer's or confluent hypergeometric function of the first kind as defined in equation (13.1.2) in Abramowitz and Stegun [1974]. We can write

$$G(x; \alpha, \lambda) = -\Gamma\left(-\frac{\alpha}{2}\right) + \Gamma\left(-\frac{\alpha}{2}\right) M\left(-\frac{\alpha}{2}, \frac{1}{2}; \frac{x^2}{2\lambda^2}\right) + \frac{2x}{\lambda\sqrt{2}} \Gamma\left(\frac{1-\alpha}{2}\right) M\left(\frac{1-\alpha}{2}, \frac{3}{2}; \frac{x^2}{2\lambda^2}\right).$$

From equation (13.1.3) in Abramowitz and Stegun [1974], the following equality holds

$$U(a, b; z) = \frac{\pi}{\sin \pi b} \left(\frac{M(a, b; z)}{\Gamma(1+a-b)\Gamma(b)} - z^{1-b} \frac{M(1+a-b, 2-b; z)}{\Gamma(a)\Gamma(2-b)} \right), \quad (\text{A.12})$$

and if we set $z = \frac{x^2}{2\lambda^2}$, $a = -\frac{\alpha}{2}$, and $b = \frac{1}{2}$, equation (A.12) becomes

$$U\left(-\frac{\alpha}{2}, \frac{1}{2}; \frac{x^2}{2\lambda^2}\right) = \pi \left(\frac{M\left(-\frac{\alpha}{2}, \frac{1}{2}; \frac{x^2}{2\lambda^2}\right)}{\Gamma\left(\frac{1-\alpha}{2}\right)\Gamma\left(\frac{1}{2}\right)} - \left(\frac{x^2}{2\lambda^2}\right)^{\frac{1}{2}} \frac{M\left(\frac{1-\alpha}{2}, \frac{3}{2}; \frac{x^2}{2\lambda^2}\right)}{\Gamma\left(-\frac{\alpha}{2}\right)\Gamma\left(\frac{3}{2}\right)} \right),$$

and since the following equalities hold

$$\begin{aligned} \left(\frac{x^2}{2\lambda^2}\right)^{\frac{1}{2}} &= \frac{|x|}{\lambda\sqrt{2}}, \\ 2\Gamma\left(\frac{3}{2}\right) &= \Gamma\left(\frac{1}{2}\right), \\ \Gamma\left(\frac{1}{2}\right) &= \pi^{\frac{1}{2}}, \end{aligned}$$

it is possible to write

$$U\left(-\frac{\alpha}{2}, \frac{1}{2}; \frac{x^2}{2\lambda^2}\right) = \frac{\pi}{k} \left(\Gamma\left(-\frac{\alpha}{2}\right) M\left(-\frac{\alpha}{2}, \frac{1}{2}; \frac{x^2}{2\lambda^2}\right) + \frac{2x}{\lambda\sqrt{2}} \Gamma\left(\frac{1-\alpha}{2}\right) M\left(\frac{1-\alpha}{2}, \frac{3}{2}; \frac{x^2}{2\lambda^2}\right) \right),$$

with

$$k = \Gamma\left(\frac{1-\alpha}{2}\right) \Gamma\left(-\frac{\alpha}{2}\right) \Gamma\left(\frac{1}{2}\right)$$

and

$$G(x; \alpha, \lambda) = -\Gamma\left(-\frac{\alpha}{2}\right) + \pi^{-\frac{1}{2}}\Gamma\left(\frac{1-\alpha}{2}\right)\Gamma\left(-\frac{\alpha}{2}\right)U\left(-\frac{\alpha}{2}, \frac{1}{2}; \frac{x^2}{2\lambda^2}\right).$$